Bled Workshops
in Physics
Vol. 18, No. 1
p. 6

Proceedings of the Mini-Workshop
Advances in Hadronic Resonances
Bled, Slovenia, July 2 - 9, 2017

The role of nucleon resonance via Primakoff effect in the very forward neutron asymmetry in high energy polarized proton-nucleus collision

I. Nakagawa for the PHENIX Collaboration

RIKEN, 2-1 Hirosawa, Wako, Saitama 351-0198, Japan

Abstract. A strikingly strong atomic mass dependence was discovered in the single spin asymmetry of the very forward neutron production in transversely polarized proton-nucleus collision at $\sqrt{s} = 200$ GeV in PHENIX experiment at RHIC. Such a drastic dependence was far beyond expectation from conventional hadronic interaction models. A theoretical attempt is made to explain the A-dependence within the framework of the ultra peripheral collision (Primakoff) effect in this document using the Mainz unitary isobar (MAID2007) model to estimate the asymmetry. The resulting calculation well reproduced the neutron asymmetry data in combination of the asymmetry comes from hadronic amplitudes. The present EM interaction calculation is confirmed to give consistent picture with the existing asymmetry results in $p^{\uparrow} + Pb \to \pi^0 + p + Pb$ at Fermi lab.

1 Nuclear Dependence of Spin Asymmetry of Forward Neutron Production

Large single spin asymmetries in very forward neutron production seen [1] using the PHENIX zero-degree calorimeters [2] are a long established feature of transversely polarized proton-proton collisions at RHIC in collision energy $\sqrt{s} = 200$ GeV. Neutron production near zero degrees is well described by the one-pion exchange (OPE) framework. The absorptive correction to the OPE generates the asymmetry as a consequence of a phase shift between the spin flip and non-spin flip amplitudes. However, the amplitude predicted by the OPE is too small to explain the large observed asymmetries. A model introducing interference of pion and a_1-Reggeon exchanges has been successful in reproducing the experimental data [3]. The forward neutron asymmetry is formulated as

$$A_N \propto \phi_{\text{flip}} \phi_{\text{non-flip}} \sin \delta \tag{1}$$

where ϕ_{flip} ($\phi_{\text{non-flip}}$) is spin flip (spin non-flip) amplitude between incident proton and out-going neutron, and δ is the relative phase between these two amplitudes. Although the OPE can contribute to both spin flip and non-flip amplitudes, resulting A_N is small due to the small relative phase. The decent amplitude can be generated only by introducing the interference between spin flip π exchange and spin non-flip a_1-Reggeon exchange which has large phase shift in between [3].

During the RHIC experiment in year 2015, RHIC delivered polarized proton collisions with gold (Au) and aluminum (Al) nuclei for the first time, enabling the exploration of the mechanism of transverse single-spin asymmetries with nuclear collisions. The observed asymmetries showed surprisingly strong A-dependence in the inclusive forward neutron production [4] and the data even change the sign of A_N from $p+p$ to $p+A$ as shown in Fig.1, while the existing framework which was successful in $p+p$ only predicts moderate A-dependence and does not have any mechanism to flip the sign of A_N in any $p+A$ collision systems [5]. Thus the observed data are absolutely unexpected and unpredicted. The $p+Au$ data point shows magnificently large A_N of about 0.18 which is three times larger than that of $p+p$ in absolute amplitude.

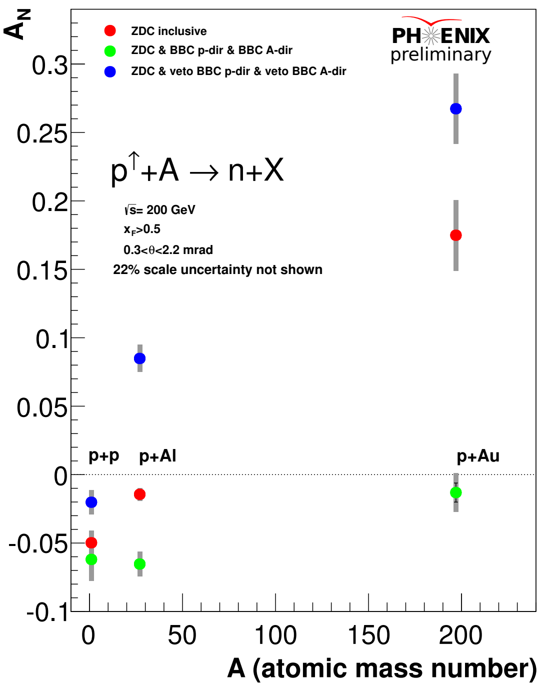

Fig. 1. (Color online) Observed forward neutron A_N in transversely polarized proton-nucleus collisions [4]. Data points are A=1, A=27, and A=197 are results of $p+p$, p+Al, and p+Au, respectively. Red, Blue and Green data points are neutron inclusive, neutron + BBC veto, and BBC tagged events, respectively.

More interestingly, another drastic dependence of A_N was observed in correlation measurements in addition to the inclusive neutron. In these measurements, another out-going charged particle was either tagged or vetoed within the acceptance of the beam-beam counter (BBC) in both North and South arms which covers $3.1 \leq |\eta| \leq 3.9$. The BBCs cover such a limited acceptance, but the resulting asymmetries behaved remarkably contradicts. Once BBC hits (BBC tagging) are required in both arms (green data points), the drastic behavior of inclusive A_N is vanished and no flipping sign was observed between $p + p$ and $p + Au$. On the contrary, the asymmetries are pushed even more positive for $p + Al$ and $p + Au$ data points once no hits in BBC are required (BBC vetoed) as represented by blue data points. Further details of the experiment are discussed in reference [4].

2 Ultra-Peripheral Collision (Primakoff) Effects

Due to the smallness of the four momentum transfers of the present kinematics, i.e. $-t \leq 0.5$ (GeV/c)^2, the EM interaction may play a role which becomes increasingly important in large atomic number nucleus. The EM field of the nucleus becomes rich source of exchanging photons between the polarized proton. This is known as the ultra-peripheral collision (UPC) in heavy ion collider experiments. In the UPC process, there is no charge exchange at the collision vertex unlike π or a_1 meson exchange.

The description of A_N is thus extended from Eq. (1) to Eqn. (2), which includes not only hadronic but also EM amplitudes:

$$A_N \propto \phi^{had}_{flip}\phi^{had}_{non-flip}\sin\delta_1 + \phi^{EM}_{flip}\phi^{had}_{non-flip}\sin\delta_2 \\ + \phi^{had}_{flip}\phi^{EM}_{non-flip}\sin\delta_3 + \phi^{EM}_{flip}\phi^{EM}_{non-flip}\sin\delta_4 \tag{2}$$

where 'EM' and 'had' stand for electromagnetic and hadronic interactions, and $\delta_1 \sim \delta_4$ are relative phases, respectively. The second and the third terms are known as Coulomb nuclear interference (CNI), which is observed to cause $< 5\%$ asymmetry of elastic scattering in $p + p$, and p+ C processes [6]. However the known asymmetry induced by the CNI is not sufficient enough to explain the present large asymmetry as large as 18%. The main focus of this document is thus the fourth term, namely the EM interference term. Before starting discussion on the EM interaction in the present neutron asymmetry, another asymmetry experiment in Fermi Lab is to be introduced in the next section.

3 Fermi's Primakoff Experiment

Here I introduce one interesting experiment which may be related with the present forward neutron asymmetry. The experiment [7] was executed in Fermi laboratory using the high energy 185 GeV transversely polarized proton beam. A large analyzing power observed in π^0 production from Pb fixed nuclear target in $|t'| < 1 \times 10^{-3}$ (GeV/c)^2 where Coulomb process is expected to play predominant role. Shown in the left panel of Fig. 2 is the invariant-mass spectrum of the $\pi^0 p$ system in $p^{\uparrow} + Pb \rightarrow \pi^0 + p +$ Pb for $|t'| < 1 \times 10^{-3}$ (GeV/c)^2. The prominent peak in region I ($W < 1.36$ GeV/c) is the $\Delta(1232)$ and the second bump is due to $N^*(1520)$ resonances. The large negative analyzing power $A_N \sim -0.57 \pm 0.12$ was observed in the region II of the invariant mass 1.36 to 1.52 GeV, while A_N was consistent with zero in the lower mass $W < 1.36$ GeV region. The authors claim this is due to the interference between the spin-flipping Δ(P33) and spin non-flipping N*(P11) resonance amplitudes as shown in the panel (a) and (b) in Fig. 3 via the Primakoff (electro-magnetic EM interaction) effect. The P11 resonance can be N*(1440) and higher resonances.

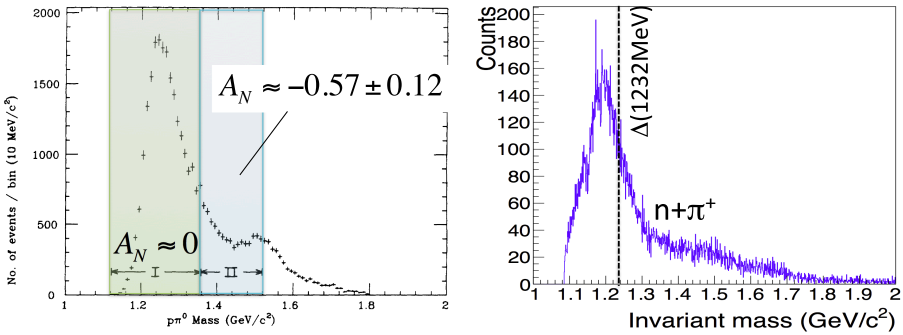

Fig. 2. (Left) The invariant-mass spectrum of the π^0 + p system in $p^\uparrow$ + Pb $\rightarrow$ π^0 + p+Pb for $|t'| < 1 \times 10^{-3}$ $(\mathrm{GeV/c})^2$ [7]. Peaks due to the $\Delta^+(1232)$ and $N^*(1520)$ resonances are shown. (Right) The Invariant mass spectrum of the Monte-Carlo simulation of the EM effect for RHIC experiment.

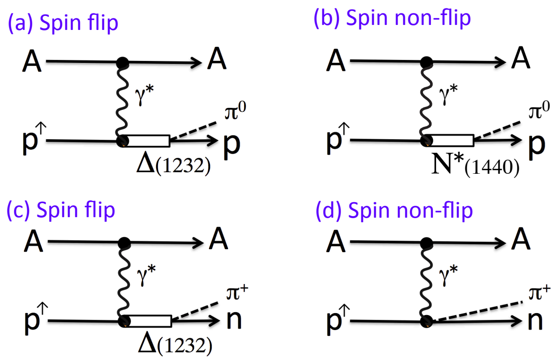

Fig. 3. The Feynman diagrams of possible spin flip and spin non-flipping amplitudes which may play key roles to produce large asymmetries in π^0 (top row) and π^+ (bottom row) productions. (d) is non-resonant π^+ production as known as Kroll-Rudermann term [14].

There are non-trivial differences between the present neutron production at RHIC and the above π^0 production at Fermi experiments. Some key experimental conditions are listed in Table 1. Due to coincidence detection of π^0 and p in the Fermi experiment, the invariant mass W of π^0p system is determined experimentally, while only neutron is detected in RHIC experiment. Therefore the invariant mass of π^+n system can only be predicted by the Monte-Carlo. Shown in the right panel of Fig. 2 is the invariant mass spectrum of π^+n system predicted by the Monte-Carlo assuming EM interaction for the RHIC experiment [10]. The nuclear photon yield is calculated by STARLIGHT model [8] while unpolarized $\gamma^* p \to \pi^+ n$ is calculated using SOPHIA model [9]. The neutron energy cut $x_F = E_n/E_p > 0.4$ is applied to be consistent with the experiment [4] where E_n is the energy of the outgoing neutron and E_p is the incident proton beam energy. As can be seen, the prominent peak is located slightly below Δ(1232MeV) peak since the equivalent photon yield is weighted to lower energy in the nuclear Coulomb field [10]. The momentum transfer are defined $t' = t - (W^2 - m^2)^2/4P_L^2$ for the Fermi experiment[1], whereas t is defined as $-t = m_n^2(1 - x_F)^2/x_F + p_T^2/x_F$ for the RHIC experiment, where m_n is neutron mass, and p_T is the transverse momentum of neutron. Unfortunately, the momentum transfers are not defined consistently between two experiments due to undetected π^+ in the RHIC experiment.

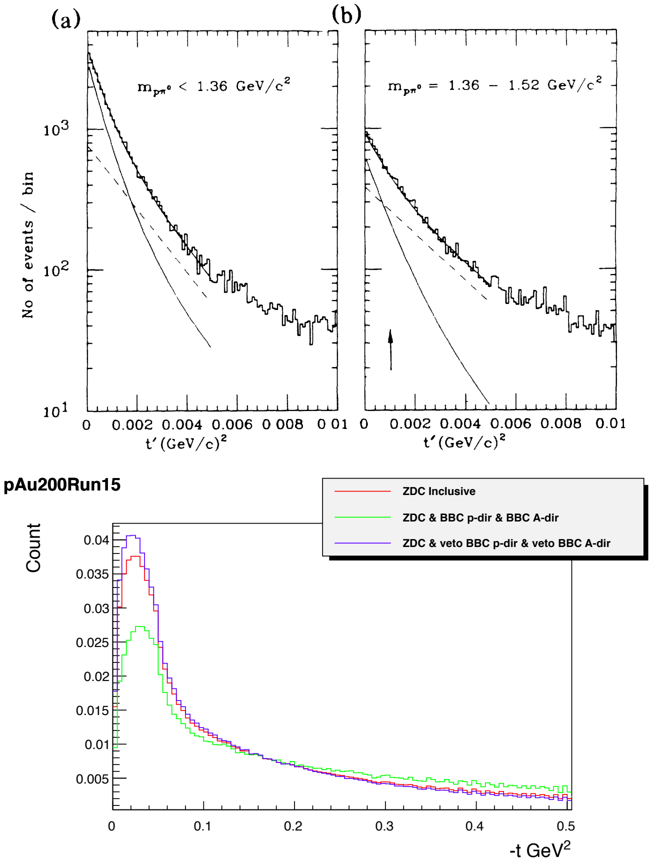

Fig. 4. (Top) The t' distributions of the $\pi^0 p$ system in $p^{\uparrow} + Pb \to \pi^0 + p + Pb$ for $W < 1.36$ GeV and $1.36 < W < 1.52$ GeV, respectively. The finite asymmetry was observed in the region $|t'| < 1 \times 10^{-3}$ (GeV/c)^2 of panel (b) [7]. (Bottom) The experimental momentum transfer distributions of the RHIC experiment for 3 different trigger selections. (Color online)

[1] See reference [7] for the definition.

Table 1. The difference of experimental conditions between RHIC [4] and Fermi [7] experiments.

	Fermi	RHIC
Beam Energy E_p [GeV]	185	100
$\sqrt{s}$ [GeV]	19.5	200
Target nucleus	Pb	Au
Detected particle(s)	$p + \pi^0$	n
Momentum transfer $(\mathrm{GeV/c})^2$	$\|t'\| < 0.001$	$0.02 < -t < 0.5$
Invariant mass W [GeV]	$1.36 < W < 1.52$	
A_N	$-0.57 \pm (0.12)_{sta} + 0.21 - 0.18$	$+0.27 \pm 0.003$

4 Asymmetry Induced by Photo-Pion Production

Pion production reaction from nucleon are intensely studied in various medium energy real photon and electron beam facilities. See reference [11] as one of review articles. The present forward neutron asymmetries via UPC effect corresponds to the photo-pion production from a transversely polarized fixed target. The polarized $\gamma^* p$ cross section is given as Eq. (4):

$$\frac{d\sigma_{\gamma^* p^\uparrow \to \pi^+ n}}{d\Omega_\pi} = \frac{|q|}{\omega_{\gamma^*}}\{R_T^{00} + P_y R_T^{0y}\} \tag{3}$$

$$= \frac{|q|}{\omega_{\gamma^*}}[R_T^{00}\{1 + P_2 \cos\phi_\pi T(\theta_\pi^*)\}] \tag{4}$$

where R_T^{00} is the unpolarized, while R_T^{0y} is target polarized response functions, respectively. $T(\theta_\pi^*)$ corresponds to the definition of the present analyzing power $A_N = T(\theta_\pi^*) = R_T^{0y}/R_T^{00}$. θ_π^* represents production angle of π in the center-of-mass system. There are several theoretical/phenomenological fitting models available to describe photo-pion production observables. Here I quote Mainz unitary isobar model, namely MAID2007 [12] to calculate the asymmetries in the present kinematics.

Shown in Fig. 5 is the MAID prediction of the unpolarized response function R_T^{00} plotted as a function of the invariant mass W of pion and nucleon systems at $Q^2 = 0(\mathrm{GeV/c})^2$ and $\theta_\pi^* = 40°$. The multipoles are weak function of $Q^2(= -t)$ and only moderately change within our kinematic coverage $-t < 0.5$ $(\mathrm{GeV/c})^2$. The leading order multipole decomposition following the notation of reference [13] is given in Eq. (5):

$$R_T^{00} = \frac{5}{2}|M_{1+}|^2 + M_{1+}^* M_{1-} + 3M_{1+}^* E_{1+} + ... \tag{5}$$

where M_{1+} is famous magnetic dipole transition amplitude from the nucleon ground state to the Δ(P33) resonance state. As blue curve indicates, the $\gamma^* p \to$

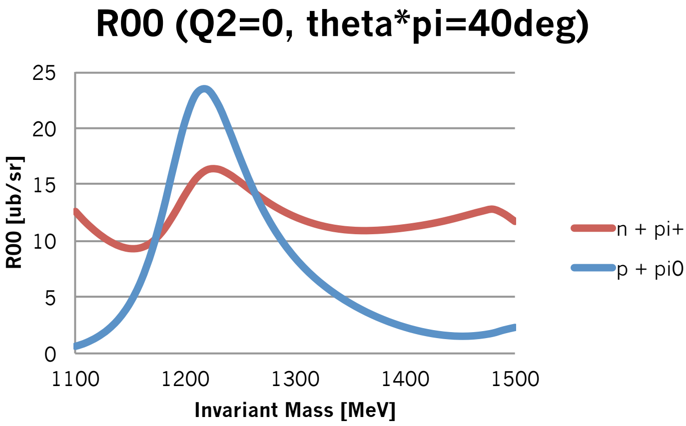

Fig. 5. (Color online) Unpolarized $R_T^{00}(W)$ response function at $Q^2 = 0(\mathrm{GeV}/c)^2$ and $\theta^*_\pi = 40^\circ$ plotted as a function of the invariant mass W [MeV]. Red and blue curves represent MAID predictions for $\gamma^* p \to \pi^+ + n$ and $\gamma^* p \to \pi^0 + p$ decay channels, respectively.

$\pi^0 p$ channel shows distinctive peak around well known Δ resonance region ($W = 1232$ MeV) in Fig. 5. This is mainly driven by the dominant $|M_{1+}|^2$ term in Eq. (5). On the contrary, the Δ peak is not as distinctive as π^0 channel for the π^+ channel and shows rather larger cross section in the threshold pion production region below Δ. This is due to enhanced charge coupling of photon to the pion field in the target proton which doesn't exist for π^0 channel. This is known as Kroll-Rudermann term [14] as shown in the diagram (d) in Fig. 3.

Shown in Fig. 6 is the target polarization response function $R_T^{0y}(W)$ of the MAID predictions for $\gamma^* p^\uparrow \to \pi^+ n$ (red) and $\gamma^* p^\uparrow \to \pi^0 p$ (blue) decay channels, respectively. The leading order multipole decomposition of R_T^{0y} is denoted as Eq. (6):

$$R_T^{0y} = \mathrm{Im}\{E^*_{0+}(E_{1+} - M_{1+}) - 4\cos\theta^*_\pi (E^*_{1+} M_{1+}) \ldots\} \tag{6}$$

The asymmetries show peak structure around Δ region for both π^+ and π^0 channels, while the sign is opposite. The magnitude of asymmetry is substantially as large as $R_T^{0y} \sim 15[\mu b/st]$ for π^+ channel compared to π^0 channel. This is because of the strong interference between E_{0+} and M_{1+} channel in π^+ channel as appears in the first term in Eqn.6. The amplitude of E_{0+} is much greater in π^+ channel compared to π^0 channel due to aforementioned Kroll-Rudermann term. Although dominant Δ amplitude, i.e. M_{1+} is even stronger in π^0 channel, this interference is relatively minor due to smallness of E_{0+} for π^0 channel.

The obtained analyzing power A_N for MAID predictions by taking the ratio of response functions $R_T^{0y}(W)$ and $R_T^{00}(W)$ are shown in Fig. 7 plotted as a function of the invariant mass W at $Q^2 = 0(\mathrm{GeV}/c)^2$ and $\theta^*_\pi = 40^\circ$. Note there are distinctive difference between π^+ and π^0 channels in A_N as a function of W according to the MAID model. π^+ shows remarkably large asymmetry over $A_N > 0.8$

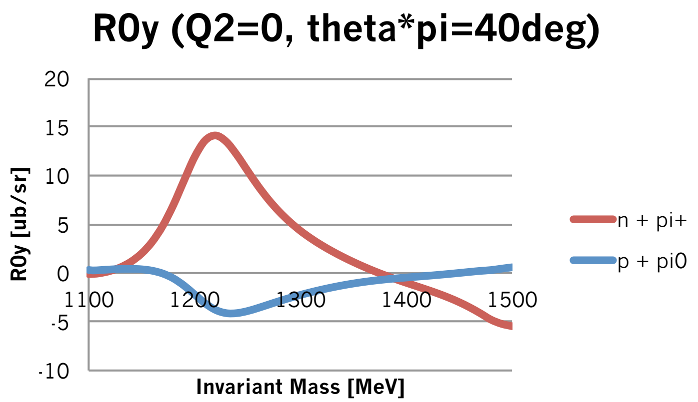

Fig. 6. (Color online) Polarized $R_T^{0y}(W)$ response function at $Q^2 = 0(\mathrm{GeV/c})^2$ and $\theta_\pi^* = 40°$ plotted as a function of the invariant mass W [MeV]. Red and blue curves represent MAID predictions for $\gamma^* p^\uparrow \rightarrow \pi^+ n$ and $\gamma^* p^\uparrow \rightarrow \pi^0 p$ decay channels, respectively.

just below Δ(1232 MeV) due to the interference between E_{0+} of Kroll-Rudermann and Δ dipole resonance M_{1+} terms. The contribution of this invariant mass region to the observed neutron is large due to matching peak of the invariant mass yield as shown in the right panel of Fig.2.

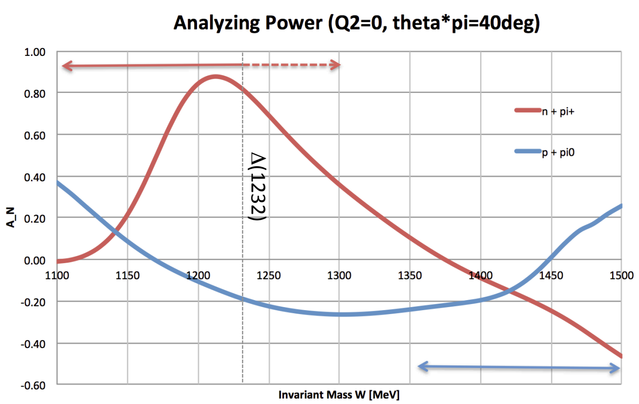

Fig. 7. (Color online) Analyzing power $A_N(W)$ at $Q^2 = 0(\mathrm{GeV/c})^2$ and $\theta_\pi^* = 40°$ plotted as a function of the invariant mass W [MeV]. Red and blue curves represent MAID [12] predictions for $\gamma^* p^\uparrow \rightarrow \pi^+ n$ and $\gamma^* p^\uparrow \rightarrow \pi^0 p$ decay channels, respectively.

The MAID is in general known to fit reasonably well to photo-pion production data in low to medium energy region. Shown in Fig. 8 is the analyzing power $T(= A_N)$ of MAID (red curve) fits to $\gamma^* p^\uparrow \rightarrow \pi^+ p$ reaction data observed in PHOENICS experiment at ELSA [15]. For the comparison, Argonne-Osaka [16] model fits are also shown in blue curve. Although some model dependence is seen in higher energies $W > 1365$ MeV in the θ^*_π region where no data, two models are fairly consistent to each other in lower energies $W < 1319$ MeV. Although the ELSA data is not necessarily perfect overlap with the kinematic range of the present RHIC data, the extrapolation of data by MAID seem to give reasonable estimate since the data coverage is sufficiently large in W bins below Δ which are rather weighted for the present neutron data.

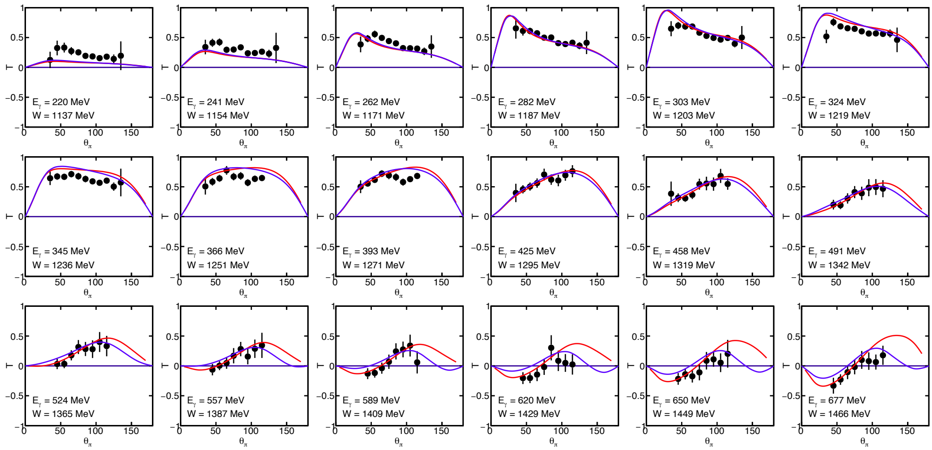

Fig. 8. (Color online) Analyzing power $T(= A_N)$ of MAID (red curve) and Argonne-Osaka [16] model (blue curve) fit to $\gamma^* p^\uparrow \to \pi^+ p$ reaction data observed in PHOENICS experiment at ELSA [15].

In reference [17], an attempt is made to evaluate average A_N within the present RHIC experiment using so evaluated MAID A_N. Shown in the left panel of the Fig.9 is the analyzing power $T(= A_N)$ as a function of pion production angle θ^*_π and the invariant mass W of $\gamma^* p^\uparrow \to \pi^+ n$. The region between thin and thick curves are the rapidity range of the present RHIC experiment and each curves corresponds to the rapidity boundaries of $\eta = 8.0$ and $\eta = 6.8$, respectively. As can be seen in the figure, the large $A_N > 0.8$ is distributed in $\theta^*_\pi < 1$ [rad] around $W \sim 1.2$ GeV and this is where the peak of the neutron yield is located as shown in the right panel of Fig.2 according to EM interaction Monte-Carlo. The yield weighted average of A_N within the acceptance between $6.8 < \eta < 8.0$ and $x_F > 0.4$ is plotted as open square in the right panel of Fig.9. The analyzing power via EM interaction are very similar between p+Al or p+Au because the slope of the photon yield as a function of photon energy is very similar. On the other hand, resulting A_N will be quite different between them due to the fraction of hadronic interaction and the EM interactions are quite different. In fact, the EM cross section grows square function of atomic number Z. The fraction of the hadronic and EM interactions are estimated by the cross section ratio of them assuming one pion exchange (OPE) for the hadronic interaction. The is simpler hadronic interaction model than the reference [5]. However, the cross section of the hadronic interaction for the leading neutron production in this very forward rapidity range $6.8 < \eta < 8.0$ is known to be dominated by OPE [3]. On the other hand, the nuclear absorption effect is claimed to play important role in the reference [5] and is not considered in reference [17] though, the absorption effects are somewhat canceled when one take ratio between the hadronic and the EM interactions. Details are discussed in the reference [17]. So obtained hadron/EM cross section weighted A_N are plotted as open circles in the right panel of Fig.9 and are compared with experimental analyzing power data (solid symbols). Solid circle and squares are inclusive and BBC vetoed data, respectively. The calculated A_N open circles are to be compared with inclusive data points (solid circle) and they are in very good agreement.

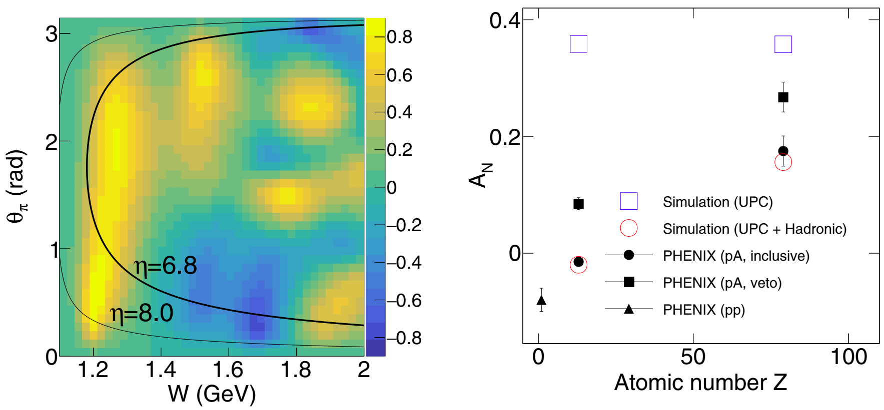

Fig. 9. (left) Analyzing power $T(= A_N)$ as a function of pion production angle in θ^*_π and the invariant mass W of $\gamma^* p^\uparrow \to \pi^+ n$. The region between thin and thick curves are the rapidity range of the present RHIC experiment and each curves corresponds to the rapidity boundaries of $\eta = 8.0$ and $\eta = 6.8$, respectively. (right) Comparison of experimental analyzing power data (solid symbols) and model predictions (open symbols) plotted as a function of atomic number Z. Solid circle and squares are inclusive and BBC vetoed data, respectively. Open square is kinematically averaged A_N prediction over RHIC acceptance by MAID. Open circles are weighted mean prediction of MAID and one pion exchange A_N for Al and Au. Both plots are quoted from reference [17].

5 Summary

A theoretical attempt was made to explain strong A-dependence in the very forward neutron asymmetry recently observed in transversely polarized proton-nucleus collision at $\sqrt{s}$=200 GeV in PHENIX experiment at RHIC [4]. The drastic A-dependence in the forward neutron asymmetry A_N cannot be explained by the conventional hadronic interaction model [5] which was successful to explain the asymmetries observed for $p + p$ collision [3]. In this document, possible major contribution in the asymmetry from the UPC (Primakoff) effect via one photon exchange from the nuclear Coulomb field is discussed. The Mainz unitary isobar (MAID2007) model [12] was used to estimate the asymmetry by the EM interaction which fit past $\gamma * p^{\uparrow} \rightarrow \pi^{+}n$ reaction data [15] well. The MAID predicts large asymmetry below Δ region for $\pi^{+}n$-channel due to the interference between non-resonance contact E_{0+} (non-spin flip) and Δ resonance M_{1+} (spin flip) amplitudes. Once kinematic average within the detector acceptance and kinematic cuts, the resulting asymmetries overshot both inclusive A_N data for both $p + Al$ and $p + Au$ data. Once these average EM asymmetries are further taken weighted mean by cross section ratio with hadronic asymmetries, the resulting asymmetries reproduced both $p + Al$ and $p + Au$ data well [17]. The importance of the interference in non-resonance and Δ resonance contradicts from the large asymmetry observed in $p^{\uparrow} + Pb \rightarrow \pi^{0} + p + Pb$ at Fermi lab [7] which is interpreted mainly due to the interference between Δ and $N^{*}(1440)$ and higher resonances. This difference can be explained by the relatively strong Kroll-Rudermann term [14] contribution for π^{+} channel, and which raises the importance of the interference below Δ unlike π^{0} channel. The present EM asymmetry calculation framework is confirmed to be at least qualitatively consistent with the claim made by the authors of Fermi experiment [7].

References

1. Y. Fukao et al., Phys. Lett. B 650, 325 (2007), A. Adare et al., Phys. Rev. D 88, 032006 (2013).
2. C. Adler, A. Denisov, E. Garcia, M. J. Murray, H. Strobele, and S. N. White, Nucl. Instrum. Methods Phys. Res., A 470, 488 (2001).
3. B. Z. Kopeliovich, I. K. Potashnikova, and Ivan Schmidt, Phys. Rev. Lett. 64, 357 (1990).
4. The PHENIX collaboration, arXiv:1703.10941.
5. B. Z. Kopeliovich, I. K. Potashnikova, and Ivan Schmidt, arXiv:1702.07708.
6. I. G. Alekseev et al.: Phys. Rev. D 79, 094014 (2009).
7. D. C. Carey et al., Phys. Rev. D 79, 094014 (2009).
8. S. R. Klein, J. Nystrand, Phys. Rev. C 60, 014903 (1999), STARLIGHT webpage, http://starlight.hepforge.org/
9. A. Mucke, R. Engel, J.P. Rachen, R.J. Protheroe, and T. Stanev, Comput. Phys. Commun. 123, 290-314 (2000); SOPHIA webpage, http://homepage.uibk.ac.at/ c705282/SOPHIA.html
10. G. Mitsuka, Eur. Phys. J. C 75:614 (2015).
11. Aron M. Bernstein, Mohammad W. Ahmed, Sean Stave, Ying K. Wu, and Henry R. Weller, Annu. Rev. Nucl. Part. Sci. 2009.59:115-144.
12. D. Drechsel, S. S. Kamalov, and L. Tiator, Unitary isobar model (MAID2007), Eur. Phys. J. A 34, 69 (2007).
13. D. Drechsel and L. Tiator, J. Phys. G: Nucl. Part Phys. **18**, 449 (1992).
14. Kroll N, Ruderman, MA. Phys. Rev. 93, 233 (1954).
15. H. Dutz et al., Nucl. Phys. **A 601**, 319 (1996).
16. H. Kamano, S. X. Nakamura, T. -S. H. Lee, and T. Sato, Phys. Rev. **C 88**, 035209 (2013).
17. G. Mitsuka, Phys. Rev. **C 95**, 044908 (2017).